



Antibacterial cellulose papers loaded with different isolated active compounds for food packaging applications

Éder Ramin de Oliveira¹ · Priscila Almeida Lucio Campini¹ · Alana Gabrieli de Souza¹ · Cristina Gomes da Silva² · Eliana Della Coletta Yudice³ · Derval dos Santos Rosa¹

Received: 17 November 2020 / Accepted: 7 June 2021 / Published online: 10 July 2021
© Iran Polymer and Petrochemical Institute 2021

Abstract

The growing trend in biodegradable and renewable materials has generated a demand for new food packaging applications. This study aimed to produce active cellulose-based papers incorporated with two different essential oil isolated active compounds, eugenol, and linalool, to promote the inhibition of pathogenic bacteria's growth. Cellulose was extracted from eucalyptus sawdust by receiving chemical and mechanical treatment and incorporating the active compounds by microwave. FTIR, SEM, TGA, DSC, and antibacterial activity against *E. coli*, *Salmonella*, *S. aureus*, and *L. monocytogenes* characterized active papers prepared by casting. Cellulose–eugenol papers showed chemical interactions by hydrogen bonding, in concern to linalool paper bands, identified by FTIR results. Highlighting that after the active compound's addition, the hydrogen energy bond values decreased from 22.5 to 22.3 kJ mol⁻¹, confirming the cellulose fibers' swelling with the oils, which slightly amorphized the papers. The active compounds changed the paper's morphology, increasing porosity and roughness, as seen in the SEM images. Besides, TGA indicated that the active compounds increased the papers' thermal resistance. The active papers exhibited excellent antimicrobial activity against all the microorganisms; the cellulose–eugenol papers demonstrated a more significant antibacterial effect (24 mm), with a larger inhibition zone than linalool paper (12 mm). These results revealed that cellulose-based papers containing eugenol or linalool have good potential to prepare antimicrobial edible papers or coatings for various types of food packaging applications.

Keywords Cellulose-based papers · Eugenol · Linalool · Food packaging · Antimicrobial properties

Introduction

Social concerns associated with the incorrect disposal of unbiodegradable plastic materials and their accumulation in the environment have increased significantly. As a reflex, food packaging industries have been looking for sustainable and renewable materials, which act as potential substitutes for commodity plastic materials (such as polypropylene and polyethylene), presenting good mechanical and thermal properties, biodegradable and renewable characteristics [1]. Cellulose is a biopolymer widely available in nature,

renewable, and low cost, which has excellent mechanical properties and is a potential substitute for food packaging preparation [2, 3].

Over the years, natural macromolecules, as cellulose fibrils or crystal, has taken different functions and applications in several segments, such as foods, medical and biomedical, packages, and others [4]. By suspending the cellulose fibrils in an aqueous medium, a network is linked by hydrogen bonding in low solid concentration, resulting in a water retention increase and a gel forming, which shows pseudoplasticity [4]. Various functions have been applied to this viscous gel, forming a dense polymeric matrix capable of store active compounds in its structure [5]. A densely packed turbid paper with high crystallinity is formed, with cellulose fibrils acting as a release controller for the active compounds [6]. Thus, this cellulosic paper is relevant material for food packaging, preserving food's quality by its antimicrobial, antioxidant properties [7].

✉ Derval dos Santos Rosa
derval.rosa@ufabc.edu.br

¹ Engineering, Modeling, and Applied Social Sciences Center (CECS), Federal University of ABC, Santo André, SP, Brazil

² Federal University of Amazonas, Manaus, AM, Brazil

³ Adolfo Lutz Institute, Santo André, SP, Brazil

In recent years, active packaging has been investigated concerning their growth potential to reduce food waste, preserve food, and avoid contamination by its antimicrobial activity, introduced by adding active agents that prevent surface growth of microorganisms and contaminations [8]. Essential oils and their isolated active compounds (ACs) are promising natural options for active packaging with antimicrobial activity. These substances are aromatic compounds obtained from specific plants generally recognized as safe (GRAS) to human consumption by the Food and Drug Administration (FDA), with a possible application as medicaments or bacterial agents [9, 10]. They are also cheaper and accessible to extract than other agents, such as silver or gold nanoparticles, previously used [11, 12].

Essential oils compose isoprene-based molecule classes, such as terpenes, terpenoids, phenolic, and aromatic compounds [13]. These molecules have a biocidal effect, acting in the disturbance of bacteria cell membrane, increasing its permeability, resulting in leakage of intracellular compounds and inducing cell destruction [13–15]. Eugenol (4-allyl-2-methoxyphenol) and linalool (3,7-dimethyl-1,6-octadien-3-ol) are examples of ACs with high bactericidal activity, being efficient against several species of Gram-positive and Gram-negative bacterial cultures [16–18]. However, essential oils are highly susceptible to degradation, oxidation, and high volatility [19]. Numerous techniques have been studied to improve ACs' applicability, such as emulsification, nanoencapsulation, among others [13–15]. Eugenol (4-allyl-2-methoxyphenol) and linalool (3,7-dimethyl-1,6-octadien-3-ol) are examples of ACs with high bactericidal activity, being efficient against several species of Gram-positive and Gram-negative bacterial cultures [17, 18, 20]. However, essential oils are highly susceptible to degradation, oxidation, and high volatility [19]. Numerous techniques have been studied to improve ACs' applicability, such as emulsification, nanoencapsulation, among others [21].

The ACs in a cellulosic matrix is an under-explored topic and of high interest since the oils can be adsorbed on the fiber surface and slowly released during the application. Muratore, Martini, and Barbosa described eugenol grafted onto cellulose papers, obtaining good biological results on repelling insects, demonstrating its applicability to food packaging [22]. Previous studies also demonstrated the ability of cellulose nanostructures as a stabilizer for essential oils with high content of eugenol and linalool, developing films with applications for antimicrobial food packaging, motivating the combination of those materials [23, 24]. Nevertheless, cellulose nanostructures can provide thermal stability and sustained release for ACs during several days, which is a good indication of the applicability of cellulosic nanostructures combined with ACs to prolong food's shelf life [17]. The ACs in a cellulosic matrix are an under-explored topic and of high interest since the oils

can be adsorbed on the fiber surface and slowly released during the application. Muratore, Martini, and Barbosa described eugenol grafted onto cellulose papers, obtaining good biological results on repelling insects, demonstrating its applicability to food packaging [22]. Previous studies also demonstrated the ability of cellulose nanostructures as a stabilizer for essential oils with high content of eugenol and linalool, developing films with applications for antimicrobial food packaging, motivating the combination of those materials [23, 24]. Nevertheless, cellulose nanostructures can provide thermal stability and sustained release for ACs during several days, which is a good indication of the applicability of cellulosic nanostructures combined with ACs to prolong food's shelf life [17].

This work's objective was to develop active cellulose papers containing two types of ACs: linalool and eugenol. Although cellulose is widely investigated and applied in several science areas, rarely publications are reported about cellulose functionalized with essential oil isolated active principles, considering AC chemical structures and their interactions with cellulose fibrils. After cellulose proceeded by ultra-Turrax and functionalized, the papers were prepared by casting method and characterized by physical–chemical interactions (FTIR), thermal stability (TGA/DSC), morphological structure (SEM), and antimicrobial (disk diffusion test) properties.

Experimental

Materials

Eucalyptus citriodora was obtained from the state of Mato Grosso (Brazil) after harvesting and cutting. Sodium chlorite was purchased from Sigma-Aldrich (SP-Brazil), and sodium hydroxide, potassium hydroxide, and chloroform were purchased from Labsynth (SP-Brazil). Linalool and eugenol oils were provided by Quinarí (PR-Brazil) and Ferquima (SP-Brazil), respectively. The purity degree of the linalool and eugenol was 99.9%.

Four microorganisms were used in this study, *Escherichia coli* (ATCC 11229), *Staphylococcus aureus* (ATCC 6538), *Listeria monocytogenes* (ATCC 19117), *Salmonella enterica* subsp. *enterica* serovar *Choleraesuis* (ATC 10708). The microorganisms were kindly donated by the Center for Interdisciplinary Procedures of Microorganisms Collection Center of Adolfo Lutz Institute (Brazil). Affiliated to World Federation Culture Collections (WFCC) #282, Depository Collection-#017/09 -SECEX/CGEN/MMA.

Methods

Preparation of cellulose fibers

The cellulose was obtained by removing the lignin and hemicellulose components, based on previous studies reported in the literature [25]. This eucalyptus sawdust (ES) was characterized and reported in a previous study already published. Its main composition is 30.2% cellulose, 28.1% lignin, 14.8% hemicellulose, 12% moisture, 7.0% ashes, and 7.0% extractives [25]. ES was previously ground and chemically treated in two steps. First, the lignin and fatty acids were removed using a sodium chloride solution (NaClO_2 , 3.8% by wt). The system was kept under stirring for 2 h at 50 °C. After this solution was filtered, washed, and dried at room temperature. In the second step, the product obtained was treated using an aqueous solution with NaOH (10% by wt) and KOH (10% by wt) under stirring, for 2 h at room temperature, washed and dried. In the second treatment, the hemicellulose and residual lignin were removed. After the treatments, the contents of the non-cellulosic components were 1.5% (by wt) hemicellulose and 2% (by wt) lignin, as previously reported by Ferreira et al. [26]. The cellulose was obtained by removing the lignin and hemicellulose components, based on previous studies reported in the literature [25]. This eucalyptus sawdust (ES) was characterized and reported in a previous study already published. Its main composition is 30.2% cellulose, 28.1% lignin, 14.8% hemicellulose, 12% moisture, 7.0% ashes, and 7.0% extractives [25]. ES was previously ground and chemically treated in two steps. First, the lignin and fatty acids were removed using a sodium chloride solution (NaClO_2 , 3.8% by wt). The system was kept under stirring for 2 h at 50 °C. After this solution was filtered, washed, and dried at room temperature. In the second step, the product obtained was treated using an aqueous solution with NaOH (10% by wt) and KOH (10% by wt) under stirring, for 2 h at room temperature, washed and dried. In the second treatment, the hemicellulose and residual lignin were removed. After the treatments, the contents of the non-cellulosic components were 1.5% (by wt) hemicellulose and 2% (by wt) lignin, as previously reported by Ferreira et al. [26].

Cellulose paper preparation

The cellulose's mechanical process was carried out using an IKA ULTRA-TURRAX® (IKA® Brazil Equipments) with dispenser tubes (model DT-20). The tube drive was filled with cellulose and distilled water, in the proportion of 0.25 g and 10 mL, respectively. The system was kept under 5000 rpm for 30 min (room temperature) to disperse the cellulose fibers and convert them into cellulose nanofibers. After that, 0.25 mL chloroform was added to the mixture and

processed for 5 min to avoid bacterial contamination during the casting process, and the solvent was evaporated after the drying process. The obtained gel was dried in Petri dishes around for three days inside a desiccator, maintained inside a chapel with air circulation at room temperature.

A similar process was conducted to prepare the active papers with ACs. After the cellulose processing, the AC volume was added, and the cellulose solution was ultrasonicated in a Sonics® Vibra Cell VCX 500 (Sonics & Materials, Inc., Connecticut, USA), with an amplitude of 50%, power of 400 W, and 24 kHz for 5 min. Figure 1 presents a scheme of the adopted methodology.

The oil volumes added to each active paper were 500 μL to eugenol and 2000 μL to linalool, aiming for good dispersion. The oil volumes were selected considering the minimum inhibitory concentration (MIC) and minimum bactericidal concentration (MBC) tests of each AC.

Characterization

Fourier-transform infrared spectroscopy

FTIR spectroscopy analyses were performed on a PerkinElmer Frontier 94942 (PerkinElmer Inc., Massachusetts, USA) using an ATR accessory. Measurements were recorded in the 500–4000 cm^{-1} , using 32 scans, at a 4 cm^{-1} .

Scanning electron microscopy

The active papers were morphologically evaluated using a Jeol-JCM 6010 Touch Scope™ microscope (Jeol, Tokyo, Japan). The device was operating with an accelerating voltage of 5 kV. Previous to the analysis, the samples were gold coated by the sputtering technique (20 nm).

Thermal analysis

TGA was performed in a PerkinElmer® STA 6000 (PerkinElmer Inc., Massachusetts, USA), applying a temperature range from 30 to 600 °C at a heating rate of 10 °C min^{-1} , in an inert atmosphere (N_2) with a flow rate of 50 mL min^{-1} .

Differential scanning calorimetry (DSC) measurements were performed using an equipment DSC Q-series (TA Instruments, Inc., Germany). The samples were heated from –50 to 200 °C at a rate of 10 °C min^{-1} under a nitrogen atmosphere (20 mL min^{-1}).

Antimicrobial assay

The antibacterial effect of the active cellulose papers without and with eugenol or linalool essential oils was determined using the disk diffusion method. Four bacterial cultures were used in this study: *Escherichia coli* (ATCC 11229),

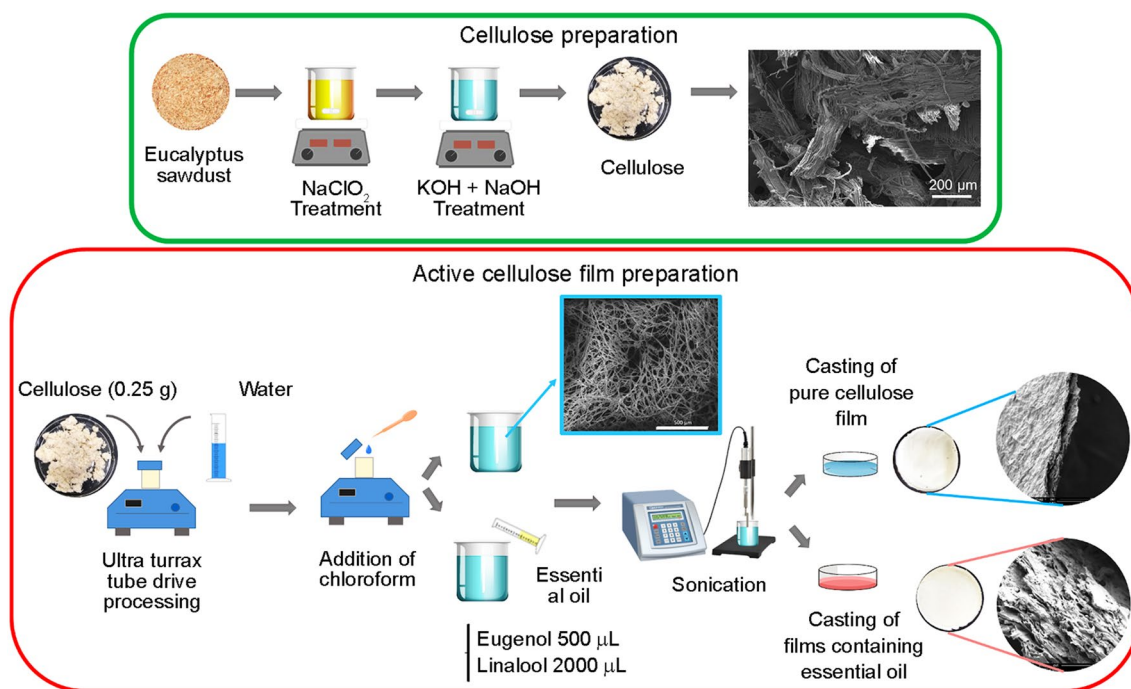


Fig. 1 Schematic representation of the adopted methodology

Salmonella enterica subsp. enterica serovar Choleraesuis (ATC 10708), *Staphylococcus aureus* (ATCC 6538), *Listeria monocytogenes* (ATCC 19117), Gram-negative (–) and Gram-positive (+), respectively.

Standard cultures were cultivated in Mueller-Hilton agar (Oxoid) and incubated at 37 °C for 24 h. The isolated suspension and standard bacterial strains were prepared from a culture made 24 h earlier, as previously described (standard turbidity: 0.5 of McFarland, standard concentration: 1.5×10^8 UFC mL⁻¹) [27]. Standard cultures were cultivated in Mueller-Hilton agar (Oxoid) and incubated at 37 °C for 24 h. The isolated suspension and standard bacterial strains were prepared from a culture made 24 h earlier, as previously described (standard turbidity: 0.5 of McFarland, standard concentration: 1.5×10^8 UFC mL⁻¹) [27].

The papers were cut into 1 cm² square and placed at the Petri disks center, incubated at 37 °C for 24 h. The experiments were conducted in triplicate for each sample and each bacterium. *Image J* software measured the diameter of inhibition zones.

Results and discussion

Fourier-transform infrared spectroscopy

FTIR verified the chemical groups of cellulose papers and essential oils and the possible interactions between both.

Figure 2 shows the spectra of all samples. The broad and main cellulose peak is at 3400–3000 cm⁻¹ (–OH stretching modes) and 2890 cm⁻¹ (aliphatic CH stretching vibrations). Furthermore, the peaks observed in the region of 1630–1620 cm⁻¹ are related to the intramolecular water molecules (O–H deformation) associated with the cellulosic fibers present in all the spectra [28]. According to Abraham et al. (2011), although all the samples were subjected to the drying process before FTIR analysis, it is still difficult to completely dry the cellulose due to the strong cellulose–water interaction. The water molecules are linked into the intramolecular structure of the fibers, limiting their removal [28]. According to Abraham et al. (2011), although all the samples were subjected to the drying process before FTIR analysis, it is still difficult to completely dry the cellulose due to the strong cellulose–water interaction. The water molecules are linked into the intramolecular structure of the fibers, limiting their removal.

Other bands, between 1500 and 800 cm⁻¹, are also specific to cellulose structure, such as 1427 cm⁻¹ (CH₂ bending), 1370 cm⁻¹ (CH₂ deformation), 1317 cm⁻¹ (–OH bending vibration), 1200 cm⁻¹, and 1162 cm⁻¹ (C–O–C asymmetric stretching mode), 1103 cm⁻¹ (–CH₂ groups), 1052 cm⁻¹ (C–O–C bonds), 1030 cm⁻¹ (vibration of C–O–C in pyranose ring), and 895 cm⁻¹ (3OH-O5 adjacent to the β-glycosidic bond of the cellulose Iα) [29, 30]. Other bands, between 1500 and 800 cm⁻¹, are also specific to cellulose structure, such as 1427 cm⁻¹ (CH₂ bending), 1370 cm⁻¹

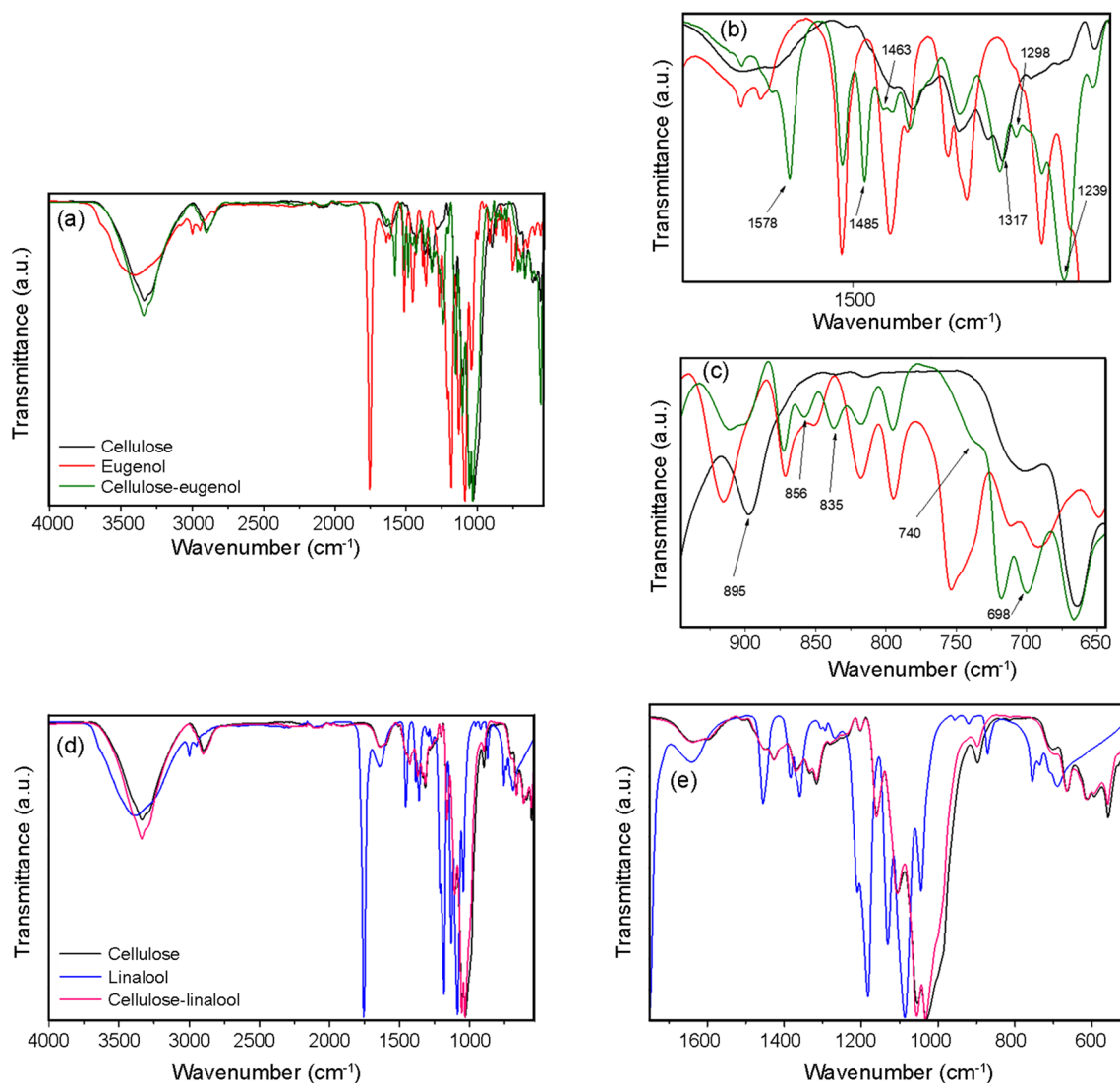


Fig. 2 FTIR spectra of cellulose papers, eugenol, and cellulose–eugenol papers: **a** full spectra; zoom in the regions, **b** 1700–1200 cm^{-1} and **c** 945–645 cm^{-1} ; and FTIR spectra of cellulose papers, linalool,

and cellulose–linalool papers: **d** full spectra; and **e** zoom in the region **b** 1700–600 cm^{-1}

(CH_2 deformation), 1317 cm^{-1} ($-\text{OH}$ bending vibration), 1200 cm^{-1} , and 1162 cm^{-1} ($\text{C}-\text{O}-\text{C}$ asymmetric stretching mode), 1103 cm^{-1} ($-\text{CH}_2$ groups), 1052 cm^{-1} ($\text{C}-\text{O}-\text{C}$ bonds), 1030 cm^{-1} (vibration of $\text{C}-\text{O}-\text{C}$ in pyranose ring), and 895 cm^{-1} ($3\text{OH}-\text{O}5$ adjacent to the β -glycosidic bond of the cellulose $\text{I}\alpha$) [29, 30].

Figure 2a presents eugenol's full-spectrum and its principal regions at 3515 cm^{-1} ; 3000 cm^{-1} ; 1800–1200 cm^{-1} ; 1000–780 cm^{-1} , which are associated with monoterpenes, aromatic ring vibrations ($\text{C}-\text{H}$, $=\text{CH}$), $\text{C}-\text{H}$ and $\text{C}-\text{O}$ stretching, and vibration of phenol $-\text{OH}$ group [31, 32]. The broad band at 3500 cm^{-1} corresponds to $-\text{OH}$ (stretching and hydrogen bond; vibrational mode) attached to an aromatic ring [33]. The bands between 2900 and 3100 cm^{-1} and 1268 and 1037 cm^{-1} are attributed to CH

stretching from aromatic groups. Besides, the bands at 1613 cm^{-1} ($-\text{C}=\text{C}-$ stretching), 1515 cm^{-1} ($\text{C}-\text{H}$ stretching), 1448 cm^{-1} ($-\text{C}-\text{C}$ deformation and CH_2 stretching in-ring), 1358 cm^{-1} (CH_3 symmetric deformation). The peaks at 1750 and 782 cm^{-1} ($\text{C}-\text{H}$ stretching) can be attributed to β -sabinene and ρ -cymene active compounds [34, 35]. Figure 2a presents eugenol's full-spectrum and its principal regions at 3515 cm^{-1} ; 3000 cm^{-1} ; 1800–1200 cm^{-1} ; 1000–780 cm^{-1} , which are associated with monoterpenes, aromatic ring vibrations ($\text{C}-\text{H}$, $=\text{CH}$), $\text{C}-\text{H}$ and $\text{C}-\text{O}$ stretching, and vibration of phenol $-\text{OH}$ group [31, 32]. The broad band at 3500 cm^{-1} corresponds to $-\text{OH}$ (stretching and hydrogen bond; vibrational mode) attached to an aromatic ring [33]. The bands between 2900 and 3100 cm^{-1} and 1268 and 1037 cm^{-1} are attributed to CH

stretching from aromatic groups. Besides, the bands at 1613 cm^{-1} ($\text{C}=\text{C}$ stretching), 1515 cm^{-1} ($\text{C}-\text{H}$ stretching), 1448 cm^{-1} ($\text{C}-\text{C}$ deformation and CH_2 stretching in-ring), 1358 cm^{-1} (CH_3 symmetric deformation). The peaks at 1750 and 782 cm^{-1} ($\text{C}-\text{H}$ stretching) can be attributed to β -sabinene and ρ -cymene active compounds [34, 35].

Cellulose–eugenol papers showed strong cellulose–eugenol chemical interaction, like hydrogen bonding, between both components. The new peaks observed at 1578 , 1485 , 1298 , and 1239 , 910 , 856 , 835 , 698 cm^{-1} , and new shoulders at 1463 and 740 cm^{-1} evidenced to represent conformational changes of cellulose or eugenol chemical structures. These peaks are found in the region associated with vibrations $\text{C}=\text{O}$, $\text{C}-\text{O}$, and $\text{C}-\text{H}$ and reflect the new chemical bond reflecting changes in the polymer chain [36]. The peaks at low wavenumbers ($<900\text{ cm}^{-1}$) represent changes in $\text{C}-\text{C}$ bonds' skeletal stretching vibration. The cellulose peaks at 1317 , 1200 , and 895 cm^{-1} showed a shift to low frequencies, correlated to the molecular order decrease due to the conformational changes [37, 38]. Cellulose–eugenol papers showed strong cellulose–eugenol chemical interaction, like hydrogen bonding, between both components. The new peaks observed at 1578 , 1485 , 1298 , and 1239 , 910 , 856 , 835 , 698 cm^{-1} , and new shoulders at 1463 and 740 cm^{-1} evidenced to represent conformational changes of cellulose or eugenol chemical structures. These peaks are found in the region associated with vibrations $\text{C}=\text{O}$, $\text{C}-\text{O}$, and $\text{C}-\text{H}$ and reflect the new chemical bond reflecting changes in the polymer chain [36]. The peaks at low wavenumbers ($<900\text{ cm}^{-1}$) represent changes in $\text{C}-\text{C}$ bonds' skeletal stretching vibration. The cellulose peaks at 1317 , 1200 , and 895 cm^{-1} showed a shift to low frequencies, correlated to the molecular order decrease due to the conformational changes [37, 38].

Figure 2d presents linalool's full spectrum. The first linalool band is around 3330 cm^{-1} attached to the functional group OH (stretching and hydrogen bond vibrational mode), and the spectrum shows weak bands in the range at $3000\text{--}2800\text{ cm}^{-1}$, correlating to monoterpene structures [39]. Another relevant region is found in the range of $1800\text{--}600\text{ cm}^{-1}$ (1752 , 1639 , 1453 , 1383 , 1356 , 1263 , 1180 , 1130 , 1083 , 1040 , 867 , 761 , and 684 cm^{-1}), and these peaks are associated with $\text{C}-\text{H}$ bending vibration, $-\text{OH}$ group, $\text{C}-\text{O}$ stretching vibration, $\text{C}=\text{H}$ stretching bonds, and $\text{C}=\text{C}$ vibrations [36, 40, 41]. Figure 2d presents linalool's full spectrum. The first linalool band is around 3330 cm^{-1} attached to the functional group OH (stretching and hydrogen bond vibrational mode), and the spectrum shows weak bands in the range at $3000\text{--}2800\text{ cm}^{-1}$, correlating to monoterpene structures [39]. Another relevant region is found in the range of $1800\text{--}600\text{ cm}^{-1}$ (1752 , 1639 , 1453 , 1383 , 1356 , 1263 , 1180 , 1130 , 1083 , 1040 , 867 , 761 , and 684 cm^{-1}), and these peaks are associated with $\text{C}-\text{H}$ bending vibration, $-\text{OH}$

group, $\text{C}-\text{O}$ stretching vibration, $\text{C}=\text{H}$ stretching bonds, and $\text{C}=\text{C}$ vibrations [36, 40, 41].

Cellulose–linalool papers showed minor changes in the FTIR spectrum concerning pristine cellulose, indicating few interactions between the components without relevant chemical bonds (Fig. 2e). This way, only slight shifts to low frequencies were observed, whereas if strong interactions between the oil and the cellulose may reflect greater retention of the oil by the matrix, delaying its release and increasing the papers' activity time.

The hydrogen bonding energy of all papers was calculated following Eq. 1, where ν_0 is the OH- standard frequency (3650 cm^{-1}), ν is the bonded OH groups frequency, and k is a constant ($1/k = 2.625 \times 10^2\text{ kJ}$) [42]:

$$E_{\text{H}} = \frac{1}{k} \left[\frac{\nu_0 - \nu}{\nu_0} \right]. \quad (1)$$

The cellulose, cellulose–eugenol, and cellulose–linalool papers showed E_{H} values of 22.5 , 22.3 , and 22.4 kJ mol^{-1} , and the reduction in the energy is a result of weakening or splitting of cellulose chains, indicating that the oils altered the cellulose cell wall structure as a result of swelling, internal fibrillation, and delamination. Besides, it is expected that a light amorphized the fibers due to the swelling process, confirming that the ACs modified cellulose papers. The oil absorption in cellulose fibrils probably diffuse into non-crystalline domains, forming new weak hydrogen bonds, and the intermolecular H-bonds are most easily affected in this case [43].

To complement these results, the Sederholm Equation was used to calculate the hydrogen bonding distance, and the results were 2.087 , 2.086 , and 2.086 \AA for cellulose, cellulose–eugenol, and cellulose–linalool papers, respectively. These results are comparable to the reported length of 0.275 nm [44].

Based on the FTIR results previously discussed, Fig. 3a shows the possible connections between cellulose and eugenol and their chemical representation in 3D. Figure 3b suggests the possible physical approximation between cellulose and linalool in terms of a chemical structure and 3D representation (*Molview* online software).

Scanning electron microscopy

Figure 4 illustrates the SEM micrographs of the mechanically processed cellulose and fractured cross-section of cellulose papers. Figures 4a, b show the cellulose's SEM after the mechanical process in the aqueous solution. A drop of the diluted solution was deposited on the support and dried. From this image, it was possible to understand the morphology of the cellulose structure after mechanical processing. The cellulose fibrils formed an interconnective

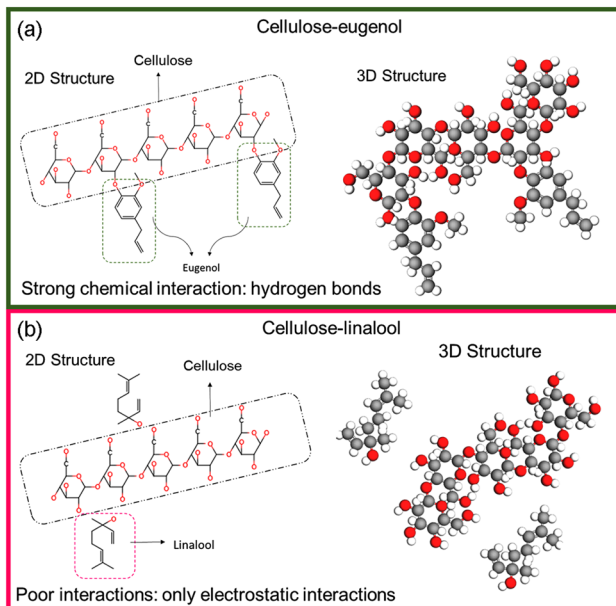


Fig. 3 Chemical structure of cellulose–eugenol and cellulose–linalool papers

porous structure that, after the solvent evaporation, leads to layers (Fig. 4c) [45]. The porous structure favors the diffusion process when the AC is added to the fibrillated cellulose structure [46], and the presence of chemical or physical interactions is responsible for the active compounds

retention, as demonstrated in the FTIR by the new hydrogen bonds formed.

The cellulose–linalool paper (Fig. 4e) is more compact and homogeneous than cellulose–eugenol, which can be justified by possible early exudation of the linalool [38]. The surface structure's roughness was more pronounced in cellulose-based papers incorporated with eugenol (Fig. 4d), which probably occurred due to the new arrangement of cellulose fibers during paper formation due to the oil's anchorage the fiber's surface [47].

Thermal analysis

Figure 5 shows cellulose papers' thermal stability without ACs, determined by TGA/DTG and DSC. Figures 5a, b show the TGA and DTG curves, respectively. From TGA curves, all samples showed a small weight loss below 100 °C resulting from the free adsorbed water [47].

In pristine cellulose papers, a single event of weight loss was observed at around 330 °C, associated with cellulose chain degradation and decomposition [48, 49]. For the papers treated with ACs, a low-intensity peak was observed between 100 and 200 °C, associated with the degradation of oily compounds [47]. The addition of the ACs slightly decreased the T_{max} of the papers. Possibly, the ACs degradation process catalyzed the thermal degradation of cellulose. However, the onset temperature of the cellulose–eugenol and cellulose–linalool paper degradation was lower than

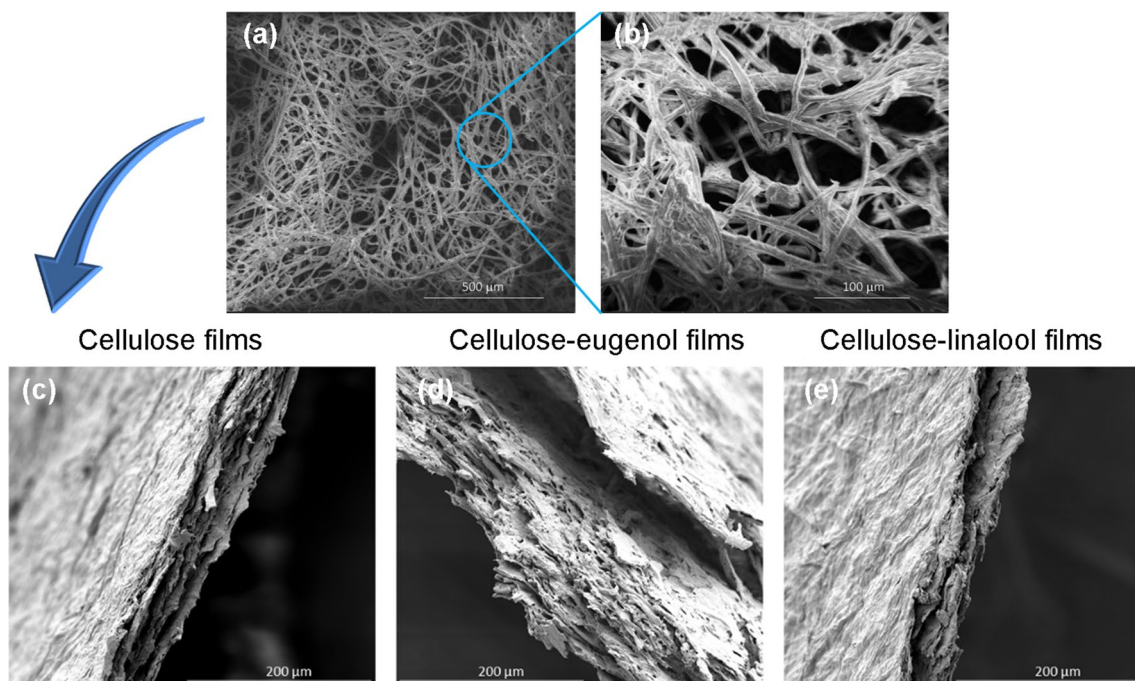


Fig. 4 SEM micrographs of **a, b** cellulose after the mechanical process (Turrax) in water solution, **c** the fractured cross-section of fibrillated cellulose papers, **d** cellulose–eugenol paper, and **e** cellulose–linalool paper

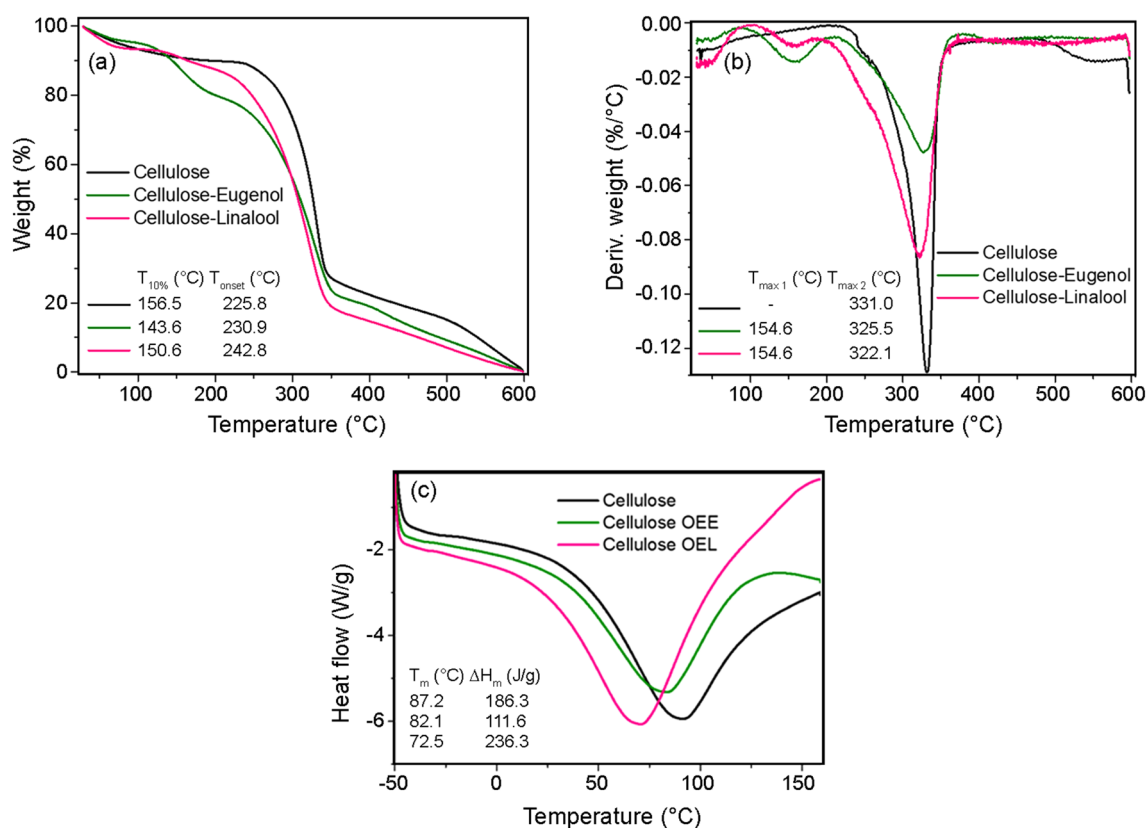


Fig. 5 Thermal analysis results of the cellulose papers and active cellulose papers with ACs. **a** TGA; **b** DTG; **c** DSC curves

in pristine cellulose papers, which can be attributed to the ACs low thermal stability. Similar behavior was noticed by Barbosa et al. [50], where Cinnamon and Ho-Wood essential oils decreased the onset temperature of neat poly(lactic acid), indicating that essential oils can reduce the onset temperature of the polymeric matrix. Still, at the same time, the matrix can offer protection for the active compounds. In pristine cellulose papers, a single event of weight loss was observed at around 330 °C, associated with cellulose chain degradation and decomposition [48, 49]. For the papers treated with ACs, a low-intensity peak was observed between 100 and 200 °C, associated with the degradation of oily compounds [47]. The addition of the ACs slightly decreased the T_{max} of the papers. Possibly, the ACs degradation process catalyzed the thermal degradation of cellulose. However, the onset temperature of the cellulose–eugenol and cellulose–linalool paper degradation was lower than in pristine cellulose papers, which can be attributed to the ACs low thermal stability. Similar behavior was noticed by Barbosa et al. [50], where Cinnamon and Ho-Wood essential oils decreased the onset temperature of neat poly(lactic acid), indicating that essential oils can reduce the onset temperature of the polymeric matrix. Still, at the same time, the matrix can offer protection for the active compounds.

Figure 5c presents the DSC thermogram of cellulose. The curve shows an endothermic peak at 87 °C, attributed to cellulose decomposition and depolymerization. The absence of an exothermic re-crystallization transition or a glass transition (T_g) suggests that these materials were predominantly crystalline [51]. The ACs addition slightly decreased the T_m values due to the oils' thermal instability that catalyze the complete cellulose degradation. The ΔH_m decreased considerably by including eugenol [52], which means that the oils can delay the thermal decomposition by reducing the amount of heat generated by the cellulose decomposition confirming the thermal stability of the papers. The increased thermal stability could be attributed to the more hydrophobic nature of the cellulosic papers with ACs [53]. However, linalool showed an opposite behavior, attributed to the poor interactions between the oil and the cellulose, as previously discussed in the FTIR results. Figure 5c presents the DSC thermogram of cellulose. The curve shows an endothermic peak at 87 °C, attributed to cellulose decomposition and depolymerization. The absence of an exothermic re-crystallization transition or a glass transition (T_g) suggests that these materials were predominantly crystalline [51]. The ACs addition slightly decreased the T_m values due to the oils' thermal instability that catalyze the complete cellulose

degradation. The ΔH_m decreased considerably by including eugenol [52], which means that the oils can delay the thermal decomposition by reducing the amount of heat generated by the cellulose decomposition confirming the thermal stability of the papers. The increased thermal stability could be attributed to the more hydrophobic nature of the cellulosic papers with ACs [53]. However, linalool showed an opposite behavior, attributed to the poor interactions between the oil and the cellulose, as previously discussed in the FTIR results.

Antimicrobial assay

The agar disc diffusion method evaluated the antibacterial activities of the cellulose papers against *E. coli* (–), *Salmonella* (–), *S. aureus* (+), and *L. monocytogenes* (+), Gram-negative (–), and Gram-positive (+), respectively. Antimicrobial activity was evaluated by measuring the inhibition zone diameter, as presented in Fig. 6. Pristine cellulose papers did not show any inhibition against four pathogenic bacteria, and the bacteria proliferated on this matrix since this biopolymer has an entirely organic and natural chemical chain, highly susceptible to microbial attack [45].

The ACs addition significantly increased the inhibition zones for all bacterial strains tested. The test results against *E. coli* bacteria are the highlight, and both ACs presented the same inhibition zone size (25.8 mm). However, the results against *S. aureus* showed a significant difference in the antibacterial activity between the two oils, cellulose–eugenol, and cellulose–linalool papers, with inhibition zones of 23.6 and 12.0 mm, respectively.

The inhibition zone size usually is related to the antimicrobial activity present in the sample or product. A larger inhibition zone usually means that the antimicrobial agent is relatively more efficient than other mediums or samples. Comparing both studied oils, the cellulose paper with eugenol AC proved to be a more effective bactericide through diameters of the halo formed (Fig. 6). Besides, eugenol essential oil demonstrated a better defined inhibition halo than linalool, which can be associated with its excellent biocidal efficiency [23]. The difference between ACs is associated with its main active agent, minimum inhibitory concentration, and interaction between the oils and fibers (which prevents its loss through evaporation).

A comparison of the antimicrobial activity against Gram-positive and Gram-negative bacteria did not reveal

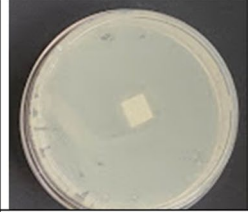
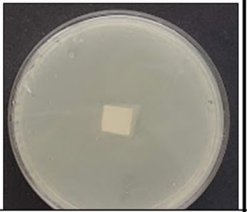
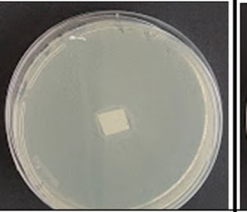
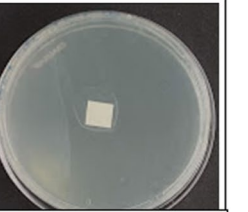
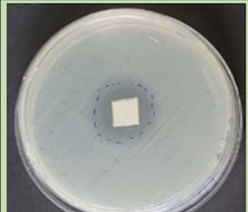

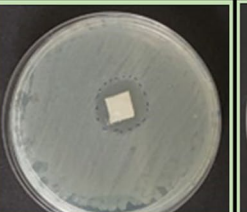
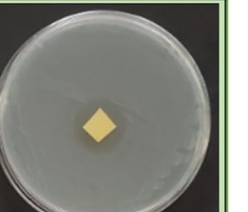
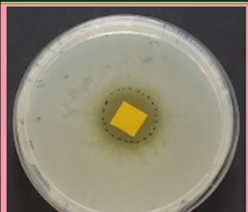
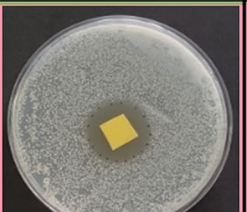
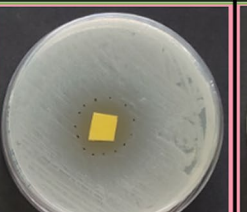
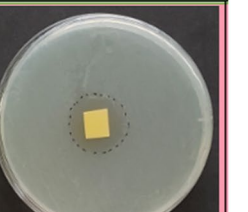
	<i>Escherichia coli</i>	<i>Staphylococcus aureus</i>	<i>Salmonella spp.</i>	<i>Listeria monocytogenes</i>
Cellulose				
Inhibition zone	0.00 mm	0.00 mm	0.00 mm	0.00 mm
Cellulose-linalool				
Inhibition zone	25.8 ± 0.1 mm	23.6 ± 0.7 mm	23.8 ± 1.2 mm	23.8 ± 1.2 mm
Cellulose-eugenol				
Inhibition zone	25.8 ± 0.1 mm	12.0 ± 0.1 mm	19.1 ± 0.1 mm	21.8 ± 1.0 mm

Fig. 6 Visual demonstration of inhibition zones for cellulose, cellulose–eugenol, and cellulose–linalool papers against *Escherichia coli* (ATCC 11229), *Staphylococcus aureus* (ATCC 6538); *Listeria mono-*

cytogenes (ATCC 19117), *Salmonella enterica* subsp. *enterica* serovar *Choleraesuis* (ATC 10708)

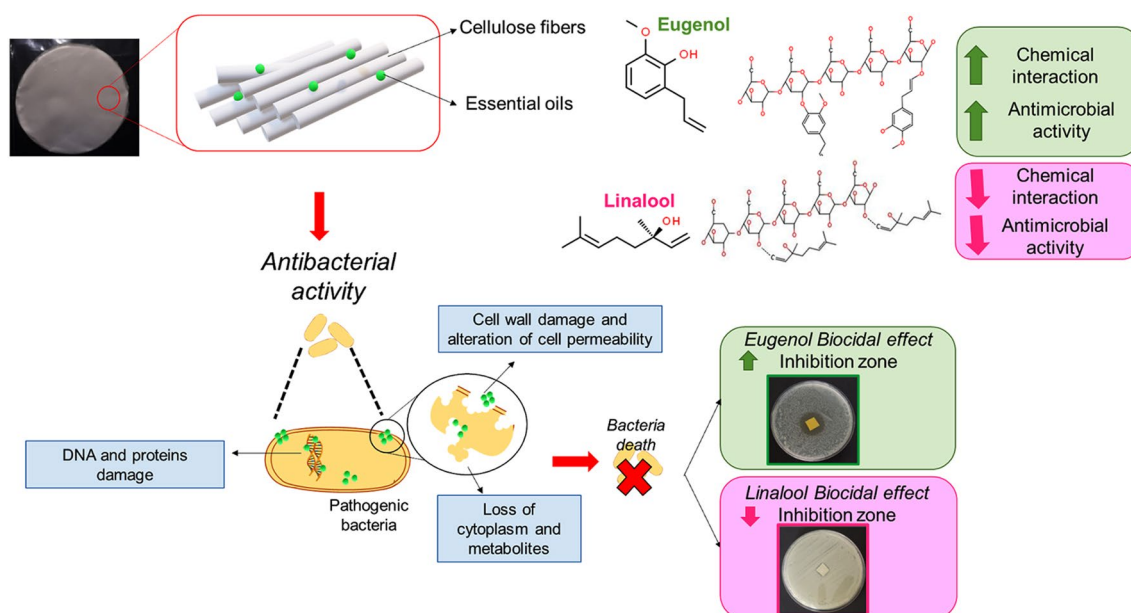


Fig. 7 Representative antimicrobial mechanisms of eugenol and linalool in the active cellulose papers

significant differences. Gram-positive bacteria have the peptidoglycan as a major component of the cell wall and a small number of proteins, while Gram-negative bacteria possess a more complex structure with various polysaccharides, proteins, and lipid-based peptidoglycan. Besides, Gram-negative has a hydrophilic membrane embedded with lipopolysaccharide molecules (phospholipid membrane) [54–56]. Our studies revealed that the papers containing eugenol and linalool have good potential against both types of bacteria. A comparison of the antimicrobial activity against Gram-positive and Gram-negative bacteria did not reveal significant differences. Gram-positive bacteria have the peptidoglycan as a major component of the cell wall and a small number of proteins, while Gram-negative bacteria possess a more complex structure with various polysaccharides, proteins, and lipid-based peptidoglycan. Besides, Gram-negative has a hydrophilic membrane embedded with lipopolysaccharide molecules (phospholipid membrane) [55, 56]. Our studies revealed that the papers containing eugenol and linalool have good potential against both types of bacteria.

Menezes et al. realized the study with seven phenylpropanoid types, i.e., the eugenol with different side groups, comparing their activity against *E. coli* medium. All structure configurations presented potential inhibition with particular MIC and MBC values. The behavior reported by each phenylpropanoid compound can be justified by their OH groups' ability to release the proton within cells based on the study presented by Joshi [57]. This process is depending on the pH medium, which facilitates the protonation of the phenolic OH group. The study proposes that the protonated phenolic compounds can quickly penetrate cells and release its proton.

These studies reported by the literature probably justify the potent antimicrobial activity efficiency of eugenol about the results of linalool inhibition in this study (Figs. 6, 7).

The antimicrobial mechanisms of essential oils' active compounds are associated with their lipophilic nature, enabling them to act on the cell membrane. First, there is an electrostatic interaction with the bacterial cell membrane, followed by the disruption of cell configuration, penetrating inside the cell, disruption of the structure of cell organelles, ion exchange, alteration of permeability, inhibition of respiration, and death [52, 54]. Figure 7 presents the main essential oil mechanisms for the biocidal effect. The antimicrobial mechanisms of essential oils' active compounds are associated with their lipophilic nature, enabling them to act on the cell membrane. First, there is an electrostatic interaction with the bacterial cell membrane, followed by the disruption of cell configuration, penetrating inside the cell, disruption of the structure of cell organelles, ion exchange, alteration of permeability, inhibition of respiration, and death [52, 54]. Figure 7 presents the main essential oil mechanisms for the biocidal effect.

Conclusion

Active cellulose papers incorporated with two different essential oils isolated active compounds (eugenol and linalool) were successfully prepared through casting method. An innovative method has been proposed since no literature has developed papers containing only cellulose fibrils and essential oils. Cellulose–eugenol papers showed excellent

chemical interaction between the AC and the matrix via hydrogen bonding, indicated by FTIR, reflected in good thermal properties and oil retention. Cellulose–linalool papers showed less chemical interaction between the oil and the matrix concerning eugenol; despite this, their thermal stability was similar to the cellulose and cellulose–eugenol papers. Cellulose fibers and active papers were organized in homogeneous layers, as seen in the SEM images. Both papers showed excellent antimicrobial properties against four pathogenic bacteria: *E. coli*, *L. monocytogenes*, *S. aureus*, and *Salmonella*. Papers with eugenol demonstrated a more significant antibacterial effect, with larger diameters and well-defined inhibition halo, associated with its excellent biocidal efficiency. The cellulose–linalool papers presented relevant results against Gram-negative bacteria, *E. coli*, and *Salmonella*, probably related to their chemical structure (linear compound) and less interaction with the cellulose matrix. The developed papers are potential candidates for active packaging in food or other sectors that require protection against disease-causing microorganisms.

Acknowledgements The authors thank the financial support provided by CNPq (#305819/2017-8; #426530/2016-0) and FAPESP (#2018/11277-7). The authors also thank UFABC, UFAM, CAPES (Code 001), REVALORES Strategic Unit, CAPES, and Multiuser Central Facilities (CEM–UFABC). The authors are grateful to the Adolfo Lutz Institute (Núcleo de Ciências Químicas e Bromatológicas–CLR/IAL–Santo André VIII, Project: CTC-09-L/2019) for his valuable contributions with bacterial tests and facilities.

Declarations

Ethics statement This study was carried out according to the recommendations and approval of the Scientific-Technical Council of the Adolfo Lutz Institute, Brazil (protocol number: CTC-IAL 09-L/2019). All subjects provided written informed consent.

References

- Chen S, Wu M, Lu P, Gao L, Yan S, Wang S (2020) Development of pH indicator and antimicrobial cellulose nanofibre packaging film based on purple sweet potato anthocyanin and oregano essential oil. *Int J Biol Macromol* 149:271–280
- Moustafa H, Youssef AM, Darwish NA, Abou-Kandil AI (2019) Eco-friendly polymer composites for green packaging: future vision and challenges. *Compos Part B Eng* 172:16–25
- Peighambaroust SJ, Zahed-Karkaj S, Peighambaroust SH, Ebrahimi Y, Peressini D (2020) Characterization of carboxymethyl cellulose-based active films incorporating non-modified and Ag or Cu-modified Cloisite 30B and montmorillonite nanoclays. *Iran Polym J* 29:1087–1097
- Dufresne A (2019) Nanocellulose processing properties and potential applications. *Curr Forest Rep* 5:76–89
- Zhang K, Wang W, Wang X, Cheng S, Zhou J, Wu Z, Li Y (2019) Fabrication and physicochemical and antibacterial properties of ethyl cellulose-structured cinnamon oil oleogel: relation between ethyl cellulose viscosity and oleogel performance. *J Sci Food Agric* 99:4063–4071
- Jahed E, Khaledabad MA, Almasi H, Hasanzadeh R (2017) Physicochemical properties of Carum copticum essential oil loaded chitosan films containing organic nanoreinforcements. *Carbohydr Polym* 164:325–338
- Rather AH, Wani TU, Khan RS, Pant B, Park M, Sheikh FA (2021) Prospects of polymeric nanofibers loaded with essential oils for biomedical and food-packaging applications. *Int J Mol Sci* 22:4017
- Khan A, Huq T, Khan RA, Riedl B, Lacroix M (2014) Nanocellulose-based composites and bioactive agents for food packaging. *Crit Rev Food Sci Nutr* 54:163–174
- Rudra SG, Gundewadi G (2020) Natural additives with antimicrobial and flavoring potential for fresh-cut produce. In: *Fresh-cut fruits and vegetables*. Elsevier, pp 165–182.
- Purkait S, Bhattacharya A, Bag A, Chattopadhyay RR (2020) Synergistic antibacterial, antifungal and antioxidant efficacy of cinnamon and clove essential oils in combination. *Arch Microbiol* 202:1439–1448
- Becerril R, Nerín C, Silva F (2020) Encapsulation systems for antimicrobial food packaging components: an update. *Molecules* 25:1134
- Akbari-Alavijeh S, Shaddel R, Jafari SM (2020) Encapsulation of food bioactives and nutraceuticals by various chitosan-based nanocarriers. *Food Hydrocoll* 105:105774
- Assadpour E, Jafari SM (2019) A systematic review on nanoencapsulation of food bioactive ingredients and nutraceuticals by various nanocarriers. *Crit Rev Food Sci Nutr* 59:3129–3151
- Guillard V, Gaucel S, Fornaciari C, Angellier-Coussy H, Buche P, Gontard N (2018) The next generation of sustainable food packaging to preserve our environment in a circular economy context. *Front Nutr* 5:1–13
- Attallah OA, Shetta A, Elshishiny F, Mamdouh W (2020) Essential oil loaded pectin/chitosan nanoparticles preparation and optimization via Box-Behnken design against MCF-7 breast cancer cell lines. *RSC Adv* 10:8703–8708
- Jin L, Liu X, Bian C, Sheng J, Song Y, Zhu Y (2020) Fabrication linalool-functionalized hollow mesoporous silica spheres nanoparticles for efficiently enhance bactericidal activity. *Chin Chem Lett* 31:2137–2141
- Lopes NA, Brandelli A (2018) Nanostructures for delivery of natural antimicrobials in food. *Crit Rev Food Sci Nutr* 58:2202–2212
- Liu X, Cai J, Chen H, Zhong Q, Hou Y, Chen W, Chen W (2020) Antibacterial activity and mechanism of linalool against *Pseudomonas aeruginosa*. *Microb Pathog* 141:103980
- Wadhwa G, Kumar S, Chhabra L, Mahant S, Rao R (2017) Essential oil–cyclodextrin complexes: an updated review. *J Incl Phenom Macrocycl Chem* 89:39–58
- Piletti R, Bugiereck AM, Pereira AT, Gussati E, Dal Magro J, Mello JMM, Dalcanton F, Ternus RZ, Soares C, Riella HG, Fiori MA (2017) Microencapsulation of eugenol molecules by β -cyclodextrine as a thermal protection method of antibacterial action. *Mater Sci Eng C* 75:259–271
- Raeisi S, Ojagh SM, Quek SY, Pourashouri P, Salaün F (2019) Nano-encapsulation of fish oil and garlic essential oil by a novel composition of wall material: Persian gum-chitosan. *LWT Food Sci Technol* 116:108494
- Muratore F, Martini RE, Barbosa SE (2018) Bioactive paper by eugenol grafting onto cellulose. Effect of reaction variables. *Food Packag Shelf Life* 15:159–168
- Han Y, Yu M, Wang L (2018) Physical and antimicrobial properties of sodium alginate/carboxymethyl cellulose films incorporated with cinnamon essential oil. *Food Packag Shelf Life* 15:35–42

24. Souza AG, Ferreira RR, Paula LC, Mitra SK, Rosa DS (2021) Starch-based films enriched with nanocellulose-stabilized Pickering emulsions containing different essential oils for possible applications in food packaging. *Food Packag Shelf Life* 27:100615
25. Silva CG, Campini PAL, Rocha DB, Rosa DS (2019) The influence of treated eucalyptus microfibers on the properties of PLA biocomposites. *Compos Sci Technol* 179:54–62
26. Ferreira RR, Souza AG, Nunes LL, Shahi N, Rangari VK, Rosa DS (2020) Use of ball mill to prepare nanocellulose from eucalyptus biomass: challenges and process optimization by combined method. *Mater Today Commun* 22:101755
27. Sarrazin SLF, Da Silva LA, Oliveira RB, Raposo JDA, Da Silva JKR, Salimena FRG, Maia JGS, Mourão RHV (2015) Antibacterial action against food-borne microorganisms and antioxidant activity of carvacrol-rich oil from *Lippia origanoides Kunth*. *Lipids Health Dis* 14:1–8
28. Le Troedec M, Sedan D, Peyratout C, Bonnet JP, Smith A, Guinebretiere R, Gloaguen V, Krausz P (2008) Influence of various chemical treatments on the composition and structure of hemp fibres. *Compos Part A Appl Sci Manuf* 39:514–522
29. Hasheminya SM, Mokarram RR, Ghanbarzadeh B, Hamishekar H, Kafil HS, Dehghannya J (2019) Influence of simultaneous application of copper oxide nanoparticles and Satureja Khuzestanica essential oil on properties of kefirán-carboxymethyl cellulose films. *Polym Test* 73:377–388
30. Khezrian A, Shahbazi Y (2018) Application of nanocomposite chitosan and carboxymethyl cellulose films containing natural preservative compounds in minced camel's meat. *Int J Biol Macromol* 106:1146–1158
31. Li Y, Kong D, Lin X, Xie Z, Bai M, Huang S, Nian H, Wu H (2016) Quality evaluation for essential oil of *Cinnamomum verum* leaves at different growth stages based on GC–MS, FTIR and microscopy. *Food Anal Method* 9:202–212
32. Li YQ, Kong DX, Wu H (2013) Analysis and evaluation of essential oil components of cinnamon barks using GC-MS and FTIR spectroscopy. *Ind Crops Prod* 41:269–278
33. da Silva CG, Kano FS, dos Santos RD (2019) Thermal stability of the PBAT biofilms with cellulose nanostructures/essential oils for active packaging. *J Therm Anal Calorim* 138:2375–2386
34. Hzounda JBF, Jazet PMD, Lazar G, Răducanu D, Caraman I, Bassene E, Boyom FF, Lazar IM (2016) Spectral and chemometric analyses reveal antioxidant properties of essential oils from four Cameroonian *Ocimum*. *Ind Crops Prod* 80:101–108
35. Schulz H, Baranska M, Belz HH, Rösch P, Strehle MA, Popp J (2004) Chemotaxonomic characterisation of essential oil plants by vibrational spectroscopy measurements. *Vib Spectrosc* 35:81–86
36. Qin Y, Li W, Liu D, Yuan M, Li L (2017) Development of active packaging film made from poly(lactic acid) incorporated essential oil. *Prog Org Coat* 103:76–82
37. Fakhreddin Hosseini S, Rezaei M, Zandi M, Ghavi FF (2013) Preparation and functional properties of fish gelatin-chitosan blend edible films. *Food Chem* 136:1490–1495
38. Ahmad M, Benjakul S, Prodpran T, Agustini TW (2012) Physico-mechanical and antimicrobial properties of gelatin film from the skin of unicorn leatherjacket incorporated with essential oils. *Food Hydrocoll* 28:189–199
39. Menezes PP, Serafini MR, Quintans-Júnior LJ, Silva GF, Oliveira JF, Carvalho FMS, Souza JCC, Matos JR, Alves PB, Matos IL, Hädärugä DI, Araújo AAS (2014) Inclusion complex of (-)-linalool and β -cyclodextrin. *J Therm Anal Calorim* 115:2429–2437
40. Bounaas K, Bouzidi N, Daghbouche Y, Garrigues S, de la Guardia M, El Hattab M (2018) Essential oil counterfeit identification through middle infrared spectroscopy. *Microchem J* 139:347–356
41. Türkoğlu GC, Sarıışık AM, Erkan G, Yıkılmaz MS, Kontart O (2020) Micro- and nano-encapsulation of limonene and permethrin for mosquito repellent finishing of cotton textiles. *Iran Polym J* 29:321–329
42. Zhao D, Deng Y, Han D, Tan L, Ding Y, Zhou Z, Xu H, Guo Y (2019) Exploring structural variations of hydrogen-bonding patterns in cellulose during mechanical pulp refining of tobacco stems. *Carbohydr Polym* 204:247–254
43. Hofstetter K, Hinterstoisser B, Salmén L (2006) Moisture uptake in native cellulose - the roles of different hydrogen bonds: a dynamic FTIR study using deuterium exchange. *Cellulose* 13:131–145
44. O'sullivan AC, (1997) Cellulose: the structure slowly unravels. *Cellulose* 4:173–207
45. Wu Y, Luo X, Li W, Song R, Li J, Li Y, Li B, Liu S (2016) Green and biodegradable composite films with novel antimicrobial performance based on cellulose. *Food Chem* 197:250–256
46. Jebel FS, Almasi H (2016) Morphological, physical, antimicrobial and release properties of ZnO nanoparticles-loaded bacterial cellulose films. *Carbohydr Polym* 149:8–19
47. Wu H, Teng C, Liu B, Tian H, Wang JG (2018) Characterization and long term antimicrobial activity of the nisin anchored cellulose films. *Int J Biol Macromol* 113:487–493
48. Arantes ACC, Silva LE, Wood DF, Almeida CG, Tonoli GHD, de Oliveira JE, da Silva JP, Williams TG, Orts WJ, Bianchi ML (2019) Bio-based thin films of cellulose nanofibrils and magnetite for potential application in green electronics. *Carbohydr Polym* 207:100–107
49. Asim M, Paridah MT, Chandrasekar M, Shahroze RM, Jawaid M, Nasir M, Siakeng R (2020) Thermal stability of natural fibers and their polymer composites. *Iran Polym J* 29:625–648
50. Barbosa RFS, Yudice EDC, Mitra SK, Rosa DS (2021) Characterization of Rosewood and *Cinnamomum cassia* essential oil polymeric capsules: stability, loading efficiency, release rate and antimicrobial properties. *Food Control* 121:107605
51. Kolakovic R, Peltonen L, Laukkanen A, Hirvonen J, Laaksonen T (2012) Nanofibrillar cellulose films for controlled drug delivery. *Eur J Pharm Biopharm* 82:308–315
52. Nisar T, Wang ZC, Yang X, Tian Y, Iqbal M, Guo Y (2018) Characterization of citrus pectin films integrated with clove bud essential oil: physical, thermal, barrier, antioxidant and antibacterial properties. *Int J Biol Macromol* 106:670–680
53. Mirzaei-Mohkam A, Garavand F, Dehnad D, Keramat J, Nasirpour A (2020) Physical, mechanical, thermal and structural characteristics of nanoencapsulated vitamin E loaded carboxymethyl cellulose films. *Prog Org Coat* 138:105383
54. Asabuwa Ngwabebhoh F, Ilkar Erdagi S, Yildiz U (2018) Pickering emulsions stabilized nanocellulosic-based nanoparticles for coumarin and curcumin nanoencapsulations: in vitro release, anticancer and antimicrobial activities. *Carbohydr Polym* 201:317–328
55. Li H, Liu Y (2019) Effects of variety and growth location on the chain-length distribution of rice starches. *J Cereal Sci* 85:77–83
56. Li X, Yang X, Deng H, Guo Y, Xue J (2020) Gelatin films incorporated with thymol nanoemulsions: physical properties and antimicrobial activities. *Int J Biol Macromol* 150:161–168
57. Joshi R (2013) Chemical composition, in vitro antimicrobial and antioxidant activities of the essential oils of *Ocimum gratissimum*, *O. sanctum* and their major constituents. *Ind J Pharm Sci* 75:457–462